

Threading dislocation lines in two-sided flux-array decorations

M.-Carmen Miguel and Mehran Kardar

Physics Department, Massachusetts Institute of Technology, Cambridge, Massachusetts 02139

(Received 13 June 1997)

Two-sided flux decoration experiments indicate that threading dislocation lines (TDL's), which cross the entire film, are sometimes trapped in metastable states. We calculate the elastic energy associated with the meanderings of a TDL. The TDL behaves as an *anisotropic and dispersive* string with thermal fluctuations largely along its Burger's vector. These fluctuations also modify the structure factor of the vortex solid. Both effects can, in principle, be used to estimate the elastic moduli of the material. [S0163-1829(97)05842-6]

Recent two-sided flux decoration experiments have proven an effective technique to visualize and correlate the positions of individual flux lines on the two sides of $\text{Bi}_2\text{Sr}_2\text{CaCu}_2\text{O}_8$ (BSCCO) thin superconductor films.^{1,2} This material belongs to the class of high- T_c superconductors (HTSC's), whose properties have drawn considerable attention in the last few years.³ Due to disorder and thermal fluctuations, the lattice of rigid lines, representing the ideal behavior of the vortices in *clean* conventional type-II superconductors, is distorted. Flux decoration allows one to quantify the wandering of the lines as they pass through the sample. The resulting decoration patterns also include different topological defects, such as grain boundaries and dislocations, which in most cases thread the entire film.

Decoration experiments are typically carried out by cooling the sample in a small magnetic field. In this process, vortices rearrange themselves from a liquidlike state at high temperatures, to an increasingly ordered structure, until they freeze at a characteristic temperature.^{4,5} Thus, the observed patterns do not represent equilibrium configurations of lines at the low temperature where decoration is performed, but metastable configurations formed at this higher *freezing temperature*. The ordering process upon reducing temperature requires the removal of various topological defects from the liquid state: Dislocation loops in the bulk of the sample can shrink, while threading dislocation lines (TDL's) that cross the film may annihilate in pairs, or glide to the edges. However, the decoration images still show TDL's in the lattice of flux lines. The concentration of defects is actually quite low at the highest applied magnetic fields \mathbf{H} (around 25G), but increases as \mathbf{H} is lowered (i.e., at smaller vortex densities). Given the high-energy cost of such defects, it is most likely that they are metastable remnants of the liquid state. (Metastable TDL's are also formed during the growth of some solid films.⁶)

Generally, a good correspondence in the position of individual vortices and topological defects is observed as they cross the sample. Nevertheless, differences at the scale of a few lattice constants occur, which indicate the wandering of the lines. Motivated by these observations, we calculate the extra energy cost associated with the deviations of a TDL from a straight line conformation. The *meandering* TDL behaves like an elastic string with a dispersive line tension which depends logarithmically on the wave vector of the distortion.

By comparing the experimental data with our results for mean-square fluctuations of a TDL, it is in principle possible to estimate the elastic moduli of the vortex lattice. Hence, this analysis is complementary to that of the hydrodynamic model of a liquid of flux lines, used so far to quantify these coefficients.¹⁰ On the other hand, the presence of even a single fluctuating TDL considerably modifies the density correlation functions measured in the decoration experiments. The contribution of the fluctuating TDL to the long-wavelength structure factor is also *anisotropic* and involves the shear modulus, making it a good candidate for the determination of this coefficient.

In the usual experimental setup, the magnetic field \mathbf{H} is oriented along to the z axis, perpendicular to the CuO planes of the superconductor. The displacements of the flux lines from a perfect triangular lattice at a point (\mathbf{r}, z) , are described in the continuum elastic limit, by a *two-dimensional* (2D) vector field $\mathbf{u}(\mathbf{r}, z)$. The corresponding elastic free-energy cost is

$$\mathcal{H} = \int \frac{d^3\mathbf{r}}{2} [c_{66}(\nabla\mathbf{u})^2 + (c_{11} - c_{66})(\nabla \cdot \mathbf{u})^2 + c_{44}(\partial_z\mathbf{u})^2], \quad (1)$$

where $\nabla = (\partial_x\hat{x} + \partial_y\hat{y})$; and c_{11} , c_{44} , and c_{66} , are the compression, tilt, and shear elastic moduli, respectively. Due to the small magnetic fields involved in the experiments, non-local elasticity effects³ are expected to be weak, and will be neglected for simplicity. In addition, at the temperatures corresponding to the freezing of decoration patterns, disorder-induced effects should be small, and will also be ignored.

To describe a dislocation line, it is necessary to specify its position within the material, and to indicate its character (edge or screw) at each point. The latter is indicated by the Burger's vector \mathbf{b} , which in the continuum limit is defined by $\oint_L d\mathbf{u} = -\mathbf{b}$, with L a closed circuit around the dislocation.¹¹ For the TDL's in our problem, the Burger's vectors lie in the xy plane, and the line conformations are generally described by the position vectors $\mathbf{R}_d(z) = \mathbf{R}(z) + z\hat{z}$ (see Fig. 1). Unlike a vortex line, the wanderings of a TDL are highly *anisotropic*: In an infinite system with a conserved number of flux lines, fluctuations of the TDL are confined to the *glide plane* containing the Burger's vector and the magnetic field. The hopping of the TDL perpendicular to its Burger's vector (*climb*) involves the creation of vacancy and interstitial lines,

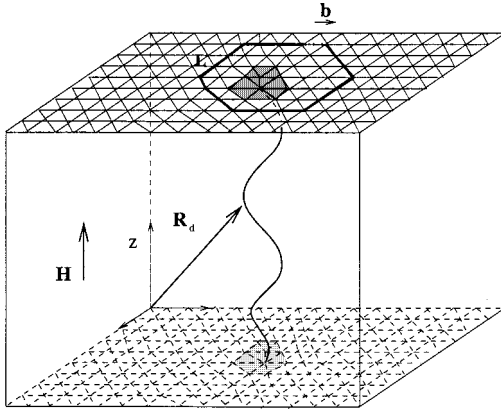


FIG. 1. Schematic plot of a TDL in a superconductor film. The Burger's vector \mathbf{b} lies in the plane perpendicular to the magnetic field \mathbf{H} .

as well as the potential crossing of flux lines.^{7,8} These defects are very costly, making the TDL climb unlikely, except, for instance, in the so-called *supersolid* phase, in which interstitials and vacancies are expected to proliferate.⁹ Nevertheless, for a sample of finite extent, introduction and removal of flux lines from the edges may enable such motion. This seems to be the case in some of the decoration experiments where the number of flux lines is not the same on the two sides.¹ In order to be completely general, at this stage we allow for the possibility of transverse fluctuations in $\mathbf{R}(z)$, bearing in mind that they may be absent due to the constraints.

We decompose the displacement field \mathbf{u} into two parts: $\mathbf{u}^s[\mathbf{r}-\mathbf{R}(z),z]$, which represents the singular displacement due to a TDL passing through points $\mathbf{R}_d(z)$ in independent two-dimensional planes; and \mathbf{u}^r , a regular field due to the couplings between the planes. By construction, the former is the solution for a two-dimensional problem with the circulation constraint,¹¹ while the latter minimizes the elastic energy in Eq. (1), and is consequently the solution to

$$c_{66}\nabla^2\mathbf{u}^r+(c_{11}-c_{66})\nabla\nabla\cdot\mathbf{u}^r+c_{44}\partial_z^2\mathbf{u}^r=-c_{44}\partial_z^2\mathbf{u}^s.$$

After Fourier transforming this equation and substituting its formal solution in Eq. (1), the energy cost of a fluctuating TDL is obtained as $\mathcal{H}^d=\mathcal{H}^{\text{str}}+\Delta\mathcal{H}$, where \mathcal{H}^{str} is the standard energy of a straight dislocation line. Keeping only the lowest order terms in the small deviations $\mathbf{R}(z)$ of the TDL axis from the straight line, gives the extra energy cost of distortions as

$$\Delta\mathcal{H}=\int\frac{dk_z}{2\pi}[A_{\perp}(k_z)|\mathbf{R}_{\perp}(k_z)|^2+A_{\parallel}(k_z)|\mathbf{R}_{\parallel}(k_z)|^2]. \quad (2)$$

Here, $\mathbf{R}(k_z)$ is the Fourier transform of $\mathbf{R}(z)$; \mathbf{R}_{\perp} and \mathbf{R}_{\parallel} stand for its components perpendicular and parallel to the Burger's vector, respectively; and

$$A_{\perp}(k_z)=\frac{b^2c_{44}}{16\pi}k_z^2\left\{\ln\left(1+\frac{c_{66}\Lambda^2}{c_{44}k_z^2}\right)+\left[2-4\frac{c_{66}}{c_{11}}+3\left(\frac{c_{66}}{c_{11}}\right)^2\right]\ln\left(1+\frac{c_{11}\Lambda^2}{c_{44}k_z^2}\right)\right\}, \quad (3)$$

$$A_{\parallel}(k_z)=\frac{b^2c_{44}}{16\pi}k_z^2\left[\ln\left(1+\frac{c_{66}\Lambda^2}{c_{44}k_z^2}\right)+\left(\frac{c_{66}}{c_{11}}\right)^2\ln\left(1+\frac{c_{11}\Lambda^2}{c_{44}k_z^2}\right)\right]. \quad (4)$$

The above expressions are obtained after integrating over \mathbf{q} , with a long-wave-vector cutoff Λ at distances of the order of the flux-line lattice spacing, below which the continuum treatment is not valid. If we also take into account a short-wave-vector cutoff Λ^* due to finite sample area, the dependence of the kernels on k_z has different forms. For values of $k_z\ll\Lambda^*\sqrt{\min(c_{66},c_{11})/c_{44}}$, the logarithms in Eqs. (3), (4) reduce to the constant value $2\ln(\Lambda/\Lambda^*)$, and both kernels are simply proportional to k_z^2 . In the opposite limit, if $k_z\gg\Lambda\sqrt{\max(c_{66},c_{11})/c_{44}}$ all the logarithms can be approximated by the first term of their Taylor expansion, and A_{\perp} and A_{\parallel} are independent of k_z . In between these extremes, the form of the kernels is globally represented through Eqs. (3), (4). In practice, the smallest wave vector k_z that can be probed experimentally is limited by the finite thickness of the sample, and is ultimately constrained (by the measured values of c_{11} , c_{66} , and c_{44}) to the last two regimes. From Eqs. (2)–(4), we conclude that the TDL behaves as an elastic string with a dispersive line tension ($\epsilon_d\propto\ln k_z$), indicating a nonlocal elastic energy. (A single flux line shows a similar dispersive behavior, as pointed out by Brandt.¹²)

Equilibrium thermal fluctuations of a TDL are calculated from Eq. (2), assuming that one can associate the Boltzmann probability $e^{-\Delta\mathcal{H}/k_B T}$ to this metastable state. After averaging over all possible configurations of $\mathbf{R}(k_z)$, the mean-square displacements are obtained as

$$\langle|\mathbf{R}_{\perp}(k_z)|^2\rangle=\frac{k_B TL}{A_{\perp}(k_z)}, \quad \text{and} \quad \langle|\mathbf{R}_{\parallel}(k_z)|^2\rangle=\frac{k_B TL}{A_{\parallel}(k_z)}, \quad (5)$$

respectively, where L is the thickness of the film. In terms of the function

$$\langle|\mathbf{R}(k_z)|^2\rangle_{c_{11}}\equiv\frac{8\pi k_B TL}{b^2c_{44}k_z^2}\ln^{-1}\left(1+\frac{c_{11}\Lambda^2}{c_{44}k_z^2}\right), \quad (6)$$

these quantities satisfy the simple relation

$$\langle|\mathbf{R}_{\perp}|^2\rangle^{-1}-\langle|\mathbf{R}_{\parallel}|^2\rangle^{-1}=\langle|\mathbf{R}|^2\rangle_{c_{11}}^{-1}\left(1-\frac{c_{66}}{c_{11}}\right)^2. \quad (7)$$

Thus, even if the TDL is allowed to meander without constraints, its fluctuations are *anisotropic*, as $A_{\perp}(k_z)=A_{\parallel}(k_z)$ only for $c_{11}=c_{66}$. In HTSC materials, $c_{66}\ll c_{11}$, so that $A_{\perp}(k_z)>A_{\parallel}(k_z)$, limiting fluctuations largely to the glide plane.

In real space, the width of the TDL depends on quantities such as $\langle|\mathbf{R}(L)|^2\rangle_{c_{11}}\equiv 1/L\int dk_z/2\pi\langle|\mathbf{R}(k_z)|^2\rangle_{c_{11}}$. Its dependence on the film thickness L follows from Eq. (6), as

$$\langle|\mathbf{R}(L)|^2\rangle_{c_{11}}\sim\frac{k_B T}{c_{11}}\begin{cases} 1/d_0 & \text{if } L\ll l_1, \\ L/\left[2l_1^2\ln\left(\frac{L}{l_1}\right)\right] & \text{if } L\gg l_1, \end{cases} \quad (8)$$

where we have defined $l_1\equiv b\sqrt{c_{44}/c_{11}}$, and d_0 is a short-distance cutoff along the z axis. For length scales below d_0 , the layered nature of the material is important.

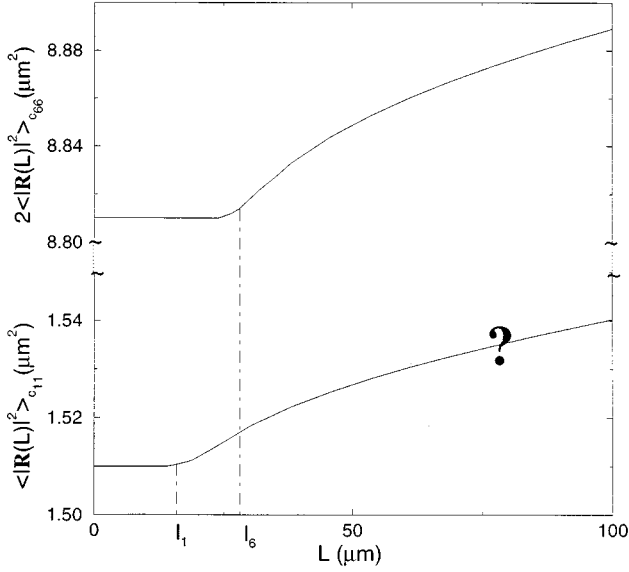


FIG. 2. Mean-square displacements as a function of the thickness L , both measured in μm , for a BSCCO sample decorated in a field of 24 G ($a_o = b = 1 \mu\text{m}$).

In order to estimate typical fluctuations for the TDL, we assume that $c_{66} \ll c_{11}$, and approximate Eq. (4) by its leading behavior. In this limit, $\langle |R_{\parallel}|^2 \rangle \approx 2\langle |R|^2 \rangle_{c_{66}}$, with $\langle |R|^2 \rangle_{c_{66}}$ defined as in Eq. (6), after replacing c_{11} with c_{66} . A behavior similar to Eq. (8) is obtained for $\langle |R|^2 \rangle_{c_{66}}$, with a corresponding crossover length $l_6 \equiv b\sqrt{c_{44}/c_{66}}$. Thus, longitudinal fluctuations of the TDL are approximately constant for samples thinner than l_6 , and grow as $L/\ln L$ for thicker samples. If allowed, transverse fluctuations follow from Eq. (7), whose leading behavior for small c_{66} gives, $\langle |R_{\perp}|^2 \rangle \sim \langle |R|^2 \rangle_{c_{11}}$. In Fig. 2 we have plotted $\langle |R|^2 \rangle_{c_{11}}$ and $2\langle |R|^2 \rangle_{c_{66}}$ as a function of the thickness L . Both quantities are very sensitive to the elastic coefficients. We have considered the values of $c_{11} = 2.8 \times 10^{-2} \text{ G}^2$, $c_{44} = 8.1 \text{ G}^2$, and $c_{66} = 9.6 \times 10^{-3} \text{ G}^2$ reported in Ref. 2 for a sample decorated in a field of 24 G, which shows a single dislocation. The Burger's vector is equal to the average lattice spacing $a_o = 1 \mu\text{m}$, and the short-distance cutoff in the plane is taken to be of the same order of magnitude. The crossover lengths introduced turn out to be $l_1 \sim 17 \mu\text{m}$, and $l_6 \sim 29 \mu\text{m}$, so that the experimental sample thickness ($L \sim 20 \mu\text{m}$) approximately falls into the constant regime in Fig. 2. From the top curve in Fig. 2, we estimate $\langle |R_{\parallel}|^2 \rangle^{1/2} \sim 3 \mu\text{m}$ for $T \sim 80 \text{ K}$, with an uncertainty factor of about $\sqrt{10}$ due to, for instance, the uncertain values of temperature, and both the in-plane and perpendicular cut-offs. If unconstrained, transverse fluctuations of the TDL are smaller, and given by $\langle |R_{\perp}|^2 \rangle^{1/2} \sim 1 \mu\text{m}$, in the same regime. The question mark in Fig. 2 is a reminder that once these fluctuations exceed a lattice spacing, proper care must be taken to account for constraints, and their violation by defects or surface effects.

As discussed in Ref. 2, the values of c_{11} and c_{66} measured in the experiments are about three orders of magnitude smaller than the theoretical predictions from Ginzburg-Landau theory. If we use the latter values in our computations, the crossover lengths become much shorter and TDL

fluctuations are reduced by three orders of magnitude. Due to this sensitivity, analysis of transverse and longitudinal fluctuations of TDL's in two-sided decoration experiments should provide a complementary method for determining the elastic moduli. Unfortunately, the films studied so far are in the short distance regime where details of the cutoff play a significant role. Experiments on thicker films are needed to probe the true continuum limit.

TDL's also produce anisotropies in the flux-line density $n(\mathbf{r}, z)$, and the corresponding diffraction patterns. Neutron-scattering studies can, in principle, resolve the full three-dimensional structure factor $S(\mathbf{q}, k_z) = \langle |n(\mathbf{q}, k_z)|^2 \rangle$, although only a few experiments are currently available for different HTSC materials.^{14,15} Two-sided decoration experiments also provide a quantitative characterization of the *two-dimensional* structure factors calculated from each surface, as well as the correlations between the two sides of the sample.

The diffraction pattern from a vortex solid has Bragg peaks at the reciprocal-lattice positions. Unbound dislocations modify the translational correlations; a finite concentration of dislocation loops can drive the long-wavelength shear modulus to zero, while maintaining the long-range orientational order.¹³ The resulting hexatic phase has diffraction rings with a sixfold modulation, which disappears in the liquid phase. In all phases, the diffuse scattering close to $\mathbf{q} = 0$ is dominated by the long-wavelength density fluctuations, which are adequately described by $n = \nabla \cdot \mathbf{u}$, leading to

$$S(\mathbf{q}, k_z) \sim \langle |\mathbf{q} \cdot \mathbf{u}(\mathbf{q}, k_z)|^2 \rangle. \quad (9)$$

The contribution of equilibrium density fluctuations (from longitudinal phonons) to Eq. (9) has the form¹⁰

$$S^o(\mathbf{q}, k_z) = \frac{k_B T L A q^2}{c_{11} q^2 + c_{44} k_z^2}, \quad (10)$$

where A is the sample area. This contribution is clearly isotropic, and independent of the shear modulus in the solid phase. (The anisotropies of the solid and hexatic phases are manifested at higher orders in \mathbf{q} .) For a sample of finite thickness, the phonon contribution in rather general situations including surface and disorder effects, was obtained in Ref. 10, as $S^o(\mathbf{q}, L) = S_{2D}^o(\mathbf{q}) R(\mathbf{q}, L)$, where $S_{2D}^o(\mathbf{q})$ is the 2D structure factor of each surface, while $R(\mathbf{q}, L)$ measures the correlations between patterns at the two sides of the film.

The above results were used in Ref. 2 to determine the elastic moduli c_{11} and c_{44} of the vortex array, at different magnetic fields. However, the decoration images used for this purpose have the appearance of a solid structure with a finite number of topological defects. We shall demonstrate here that the presence of a single trapped TDL modifies the isotropic behavior in Eq. (10). We henceforth decompose the displacement field $\mathbf{u}(\mathbf{r})$ into a *regular* phonon part \mathbf{u}^o , and a contribution $\mathbf{u}^d = \mathbf{u}^s + \mathbf{u}^r$ from the meandering TDL described by $\mathbf{R}(z)$. The overall elastic energy also decomposes into independent contributions $\mathcal{H}[\mathbf{u}^o, \mathbf{R}] = \mathcal{H}^o[\mathbf{u}^o] + \mathcal{H}^d[\mathbf{R}]$. To calculate the average of any quantity, we integrate over smoothly varying displacements \mathbf{u}^o , and over distinct con-

figurations of the dislocation line $\mathbf{R}(z)$. Thus the structure factor in Eq. (9) becomes a sum of *phonon* and *dislocation* parts.

The results of Eq. (5) can be used to calculate the contribution from a fluctuating TDL, which has the form

$$S^d(\mathbf{q}, k_z) = \frac{8\pi L b^2 c_{66}^2 q_{\perp}^2}{c_{11}^2 q^4} \delta(k_z) + \frac{k_B T L b^2}{(c_{11} q^2 + c_{44} k_z^2)^2} \times \left(\frac{4c_{66}^2 q_{\parallel}^2 q_{\perp}^2}{A_{\parallel}(k_z)} + \frac{(c_{44} k_z^2 + 2c_{66} q_{\perp}^2)^2}{A_{\perp}(k_z)} \right), \quad (11)$$

$q_{\parallel} \equiv \mathbf{q} \cdot \mathbf{b}/b$, and q_{\perp} the component perpendicular to the Burger's vector. The first term on the right-hand side (rhs) of Eq. (11) corresponds to the straight TDL, and vanishes in the liquid state with $c_{66} = 0$. The next two terms on the rhs result from the longitudinal and transverse fluctuations of the TDL, respectively. (The latter is absent if the TDL is constrained to its glide plane.) The *dislocation* part is clearly anisotropic, and the anisotropy involves the shear modulus c_{66} . Thus after inverting the k_z transform in Eq. (11), the TDL contribution to the structure factors calculated from the two-sided decoration experiments can also be exploited to obtain information about the elastic moduli.

In conclusion, we have calculated the energy cost of meanderings of a TDL in the flux lattice of a HTSC film such as

BSCCO. Flux decoration experiments indicate that such metastable TDL's are indeed frequently trapped in thin films in the process of field cooling. We have estimated the thermal fluctuations of a TDL in crossing the sample, as well as its contribution to the structure factor. Both effects can, in principle, be used to estimate the elastic moduli of the vortex solid. However, there are strong interactions between such defects, which need to be considered when a finite number of TDL's of different Burger's vectors are present. The generalization of the approach presented here to more than one TDL may provide a better description of the experimental situation. From the experimental perspective, it should be possible to find samples with a single trapped TDL, providing a direct test of the theory. Other realizations of TDL's can be found in grown films,⁶ and may also occur in smectic liquid crystals. It would be interesting to elucidate the similarities and distinctions between the defects in these systems.

M.C.M. acknowledges financial support from the Direcció General de Recerca (Generalitat de Catalunya). M.K. is supported by the NSF Grant No. DMR-93-03667. We are grateful to D.R. Nelson for emphasizing to us the constraints on transverse motions of TDL's. We have benefited from conversations with M.V. Marchevsky, and also thank Z. Yao for providing us with the raw decoration images from Refs. 1 and 2.

¹Z. Yao *et al.*, Nature (London) **371**, 777 (1994).

²S. Yoon *et al.*, Science **270**, 270 (1995).

³G. Blatter *et al.*, Rev. Mod. Phys. **66**, 1125 (1994).

⁴D. Grier *et al.*, Phys. Rev. Lett. **66**, 2270 (1991).

⁵M. V. Marchevsky, Ph.D. thesis, Leiden University, 1997.

⁶E. A. Fitzgerald, Mater. Sci. Rep. **7**, 87 (1991).

⁷R. Labusch, Phys. Lett. **22**, 9 (1966).

⁸F. R. N. Nabarro and A. T. Quintanilha, in *Dislocations in Solids*, edited by F. R. N. Nabarro (North-Holland, Amsterdam, 1980), Vol. 5.

⁹E. Frey, D. R. Nelson, and D. S. Fisher, Phys. Rev. B **49**, 9723 (1994).

¹⁰M. C. Marchetti and D. R. Nelson, Phys. Rev. B **47**, 12 214 (1993); *ibid.* **52**, 7720 (1995).

¹¹L. D. Landau and E. M. Lifschitz, *Theory of Elasticity* (Pergamon, New York, 1970).

¹²E. H. Brandt, J. Low Temp. Phys. **26**, 735 (1977).

¹³M. C. Marchetti and D. R. Nelson, Phys. Rev. B **41**, 1910 (1990).

¹⁴R. Cubbit *et al.*, Nature (London) **365**, 407 (1993).

¹⁵U. Yaron *et al.*, Phys. Rev. Lett. **73**, 2748 (1994).